RSC Advances

ROYAL SOCIETY OF CHEMISTRY

www.rsc.org/advances

A table of contents entry

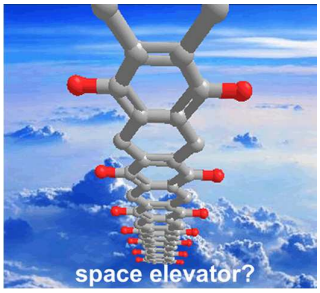

All-carbon ladder polymer with high modulus and high structural similarities to graphene nanoribbons is synthesized by a facile one-pot method.

RSC Advances

RSCPublishing

ARTICLE

High-Modulus All-carbon Ladder Polymer of Hydroquinone and Formaldehyde that Bridges the Gap between Single Strand Polymers and Graphene Nanoribbons

Cite this: DOI: 10.1039/x0xx00000x

Received ooth January 2012,
Accepted ooth January 2012

DOI: 10.1039/x0xx00000x

www.rsc.org/

Shao-Zhong Zeng, [a,d] Neng-Zhi Jin, [b] Hai-Lu Zhang, [b] Bin Hai, [a] Xiao-Hua Chen, [a] and Jianlin Shi*[,d]

The high strength and novel electronic properties of all-carbon macromolecules, as represented by carbon nanotubes and graphenes, are originated from their conjugated all-carbon structures. The synthetic polymers with conjugated all-carbon ladder structures would partially inherit the excellent properties of carbon nanotubes and graphenes. These polymers, such as polyacene (PAC), however, are especially difficult in synthesis. Here, we demonstrate the facile synthesis of all-carbon straight ladder polymer from a one-pot polycondensation reaction between hydroquinone and formaldehyde. This polymer could be oxidized and isomerized into a fully aromatic all-carbon ladder structure identical to that of PAC. Such a conjugated all-carbon ladder structure will provide a long-sought model for the investigations on the mechanical and electronic properties of PAC-like ladder structures. The chain modulus and skeleton modulus of this polymer were calculated to be up to 50 (528 GPa) and 89 (932 GPa) percents of that of CNT(5,5) (1046 GPa), respectively.

Introduction

The extremely high Young's moduli up to 1.0 TPa of single-walled carbon nanotubes (SWCNTs) and graphene nanoribbons (GNRs) are currently thought to be the insurmountable upper limit to other synthetic polymers.[1-5] Great efforts have been devoted to synthesizing polymers with Young's moduli close to this limit, but only half of the limit has been reached by the stiffest synthetic polymers reported so far.[6, 7]

Regarding the SWCNTs and GNRs as the limiting cases of synthetic polymers, *i.e.*, all-carbon macromolecules, there are a large gap between the SWCNTs/GNRs and the synthetic polymers in both structures and performances. There are a number of conjugated carbon strands in SWCNTs and GNRs while only one carbon strand is present in most of the synthetic polymers except for ladder polymers.[8, 9] Ladder polymers have been proposed as: "polymers consists of two independent strands connected via rigid bridges without formation of crossing-points, e.g. double bonds or spiro centers."[10] Among the various ladder polymers, polymers with winding configurations [11, 12] are unqualified as high modulus polymers because the winding macromolecular chains could be easily stretched through bending the chemical bonds. Therefore, only the polymers with linear configuration could have high modulus. Polyacene (PAC) is the simplest linear ladder polymer constructed solely with laterally fused benzene rings and could be regarded as the narrowest GNR.[13, 14] Owing to the structural similarity between PAC and GNRs, the skeleton of PAC could have extremely high modulus comparable to that of GNRs (ca. 1.0 TPa). Unfortunately, it has been shown that PAC is extremely unstable and very difficult to synthesize,[13,14] only oligoacene with up to nine benzene rings has been carefully synthesized.[15] Though all-carbon ladder backbone as perfect as PAC has not been reported so far due to the difficulties in its synthesis, two other kinds of polymers with similar structures to PAC have been reported. One is the fully unsaturated all-carbon ladder polymers,[9, 16] the other is the heteroaroatic ladder polymers.[17] However, these polymers could not be made into reinforcements because of the larger side groups or the poor solubility.

The condensation reactions between para-substituted phenols and formaldehyde are known to produce linear polymers or calixarenes (Fig. 1A).[18, 19] Specially, let the para-substituted group be hydroxyl group, what would happen in the reaction between

RSC Advances

RSCPublishing

ARTICLE

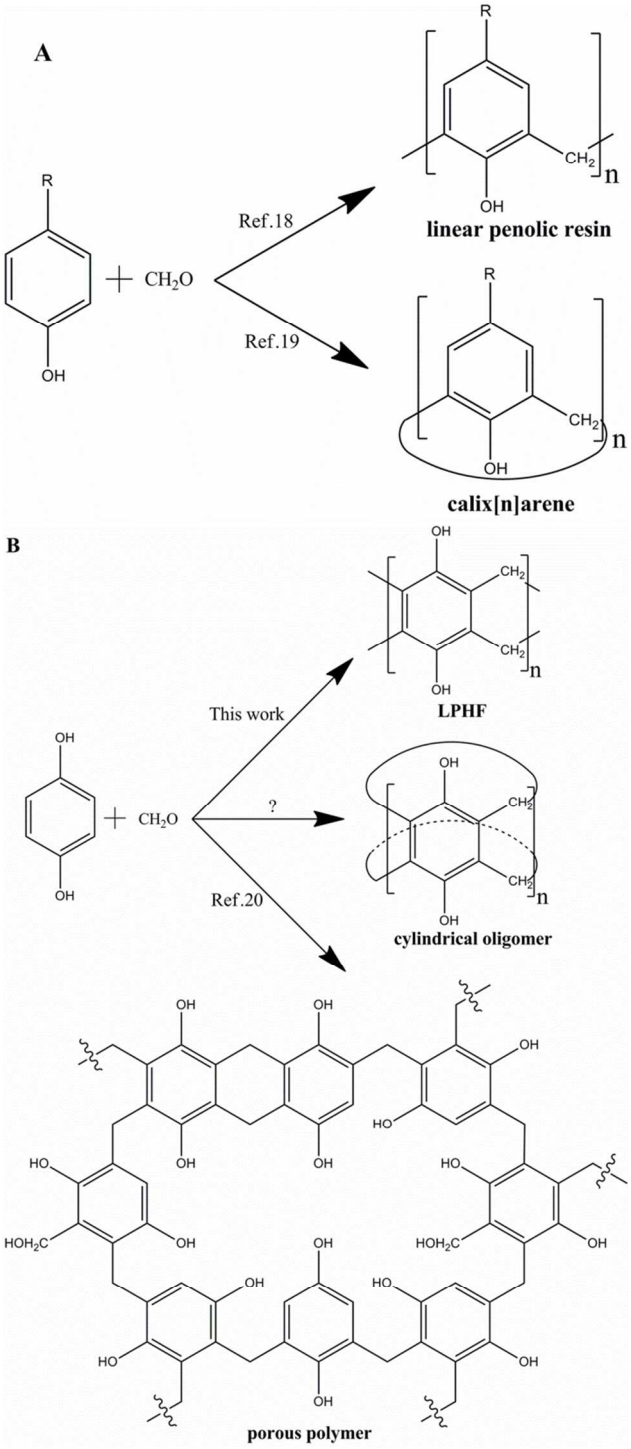

Fig. 1 Reaction schematics between para-substituted phenol and formaldehyde (A) producing linear polymers and calix[n]arenes; Those between hydroquinone and formaldehyde (B) producing ladder polymer, cylindrical oligomer or porous polymer. For clarity, CH_2 was not labeled in the porous polymer.

hydroquinone and formaldehyde? In addition to the porous polymer previously reported by us,[20] could the reaction yield coplanar ladder polymer or cylindrical oligomers (Fig. 1B)? The ladder polymer with one defect (monosubstituted methylene) for 8~9 repeat units has been reported by M. H. Litt.[21] Here, we report the synthesis of nanoribbons composed of oriented ladder polymer chains (Fig. 1B). The ladder polymer of hydroquinone and formaldehyde (LPHF) was confirmed to have a straight coplanar ladder structure by TEM, NMR and Raman spectrum. The backbone of LPHF is highly similar to that of PAC except for the bond order of the carbon-carbon bonds. Furthermore, the backbone of LPHF can be oxidized and isomerized to fully aromatic all-carbon ladder backbone.[21] This ladder backbone is totally the same as that of PAC. The orientation of the macromolecular chains results in the formation of nanoribbons with a Brunauer-Emmett-Teller (BET) surface area up to 115 $m^2 g^{-1}$ (Fig. S1).[22] The chain modulus of LPHF calculated with Gaussian 09 is as high as 528 GPa,[23] which is close to those of polypyridobisimidazole (PIPD, 543 GPa) and poly(p-phenylenebenzobisoxazole) (PBO, 530 GPa).[6, 7] The presence of numerous hydroxyl groups on the edges of the nanoribbons implies that such a kind of LPHF nanoribbons could strongly interact with other polar polymer matrices. This strong interaction together with its high surface area and high modulus, qualifies its application in reinforcing other polymer matrices.

Experimental section

Materials

Hydroquinone (AR, 99%), formaldehyde (AR, 37 wt%), concentrated hydrochloric acid (AR, 37 wt%), silver nitrate (AR, 99.8%), ammonium hydroxide (AR, 35%) and sodium borohydride (96%) were purchased from Shanghai Chemical Reagent Plant (Shanghai, PR China) and were used as received.

Synthesis of LPHF

hydroquinone (1.65 g, 0.015 mol), 2.5 mL 37wt% formaldehyde and 125 mL 10wt% hydrochloric acid was mixed and dissolved in a 200 mL autoclave with Teflon lining. Then the autoclave was sealed and heated in an oven at 180 ^oC for 12 h. The resulting black sponge-like product was filtrated and washed with water. The filter cake was vacuum dried at 60 ^oC for 6 h. Finally, 2.0 g lightweight and dark brown powder was collected. The yield was close to the quantitative (based on hydroquinone).

$NaNH_4$ Treatment

0.30 g LPHF was soaked in the solution of 1g $NaBH_4$ and 45 g ethanol. The mixture was treated on an ultrasonic oscillator for 1 h. Then 30 g 10wt% HCl was added into the mixture under vigorous agitation. The solid product was centrifuged and thoroughly washed with water. The product was vacuum dried at 60 ^oC for 6 h.

LPHF oxidation with $Ag(NH_3)_2^+$

The ammoniacal silver nitrate solution was prepared according to the following procedure: 2 M $NH_3 \cdot H_2O$ was dropped into the solution of 1.7010 g (10 mmol) $AgNO_3$ and 15 g water till the precipitates just dissolved. This solution (pH=9.8) was diluted with ammonia (pH=9.8) to 100 mL.
0.05g LPHF was soaked in 20 mL 0.1 mol/L $Ag(NH_3)_2^+$ solution and stirred at 25 ^oC for 24 h. The solid was isolated by centrifugation and dried. 0.13 g composite of OLPHF-Ag was collected.

Characterizations

^{13}C NMR experiments were performed with 4 mm double-resonance MAS probe on a Bruker AVANCE III-500 spectrometer operating at a magnetic field strength of 11.7 T. A total sideband suppression (TOSS) frame was embedded into the conversional Cross-Polarization (CP) pulse sequence,[24] which was used to acquire the ^{13}C CP/MAS spectra. The Harmann-Hahn condition was optimized by using adamantane. ^{13}C CP/MAS NMR spectra were obtained at an 8 kHz MAS spinning speed with a 2 ms contact time and a 6 s recycle delay. The chemical shifts were externally referenced to tetramethylsilane (TMS, 0 ppm).
Powder X-ray diffraction (XRD) patterns were recorded on a Rigaku D/MAX-2250V diffractometer using Cu Kα radiation (40 kV and 40 mA). Data was collected from $2\theta = 10^o$ to 80^o in a step of 0.02^o with a scanning rate of 8^o/min.
The nitrogen isotherms were measured at 77 K using an ASAP 2010 (Micromeritics Co.). The samples were pretreated at 393 k under nitrogen flow for 12 h. The specific surface area (S_{BET}) was calculated using the Brunauer-Emmett-Teller (BET) method based on adsorption data in the partial pressure (P/P_o) range 0.05-0.20.

Calculations

All the quantum chemistry calculations were performed on a high-performance machine using the density functional theory (DFT) approach in Gaussian 09.[23] Oligomer extrapolation method was used for predicting NMR shielding tensors due to the limitation of Gaussian 09. The chemical shielding parameters were calculated with the Gauge-Independent Atomic Orbital (GIAO) method. The theoretical chemical shifts were calculated with HF/6-311+G(2d,p) on structures optimized with B3LYP/6-31G(d).[25, 26] The chemical shifts were obtained from the differences between the ^{13}C shielding results of tetramethylsilane (TMS) and those of oligomers. The center-most unit best represents the unit in infinite polymer. Therefore, the average chemical shifts of carbon atoms in the center-most unit are close to that in real polymer. The results also demonstrate that the theoretical chemical shifts of these oligomers with 3 ~ 6 repeat units are almost constant, which proves the validity of the oligomer extrapolation method.
Oligomer with ten hydroquinone units was chosen to be a calculation model because its vibration modes were close to the modes of infinite long polymer. Raman spectrum was calculated with PBEPBE/6-31G(d) on the structure optimized with PBEPBE/6-31G(d).[27] All the calculated vibration frequencies were scaled by 0.986. The calculated Raman spectrum was broadened by convoluting the calculated Raman lines with a Gaussian having a fwhm (full width at half maximum) of 50 cm^{-1}.
The chain moduli for all polymers were calculated from the second order derivative of the total energy curve.[7] The total energy curve were obtained with PBEPBE/6-31G(d) from the total energy scanning along the length of structural unit (lattice translation vector). First of all, the structural units were optimized with PBEPBE/6-31G(d) to get the ground-state units and the ground-state energy. The ground-state energy of all molecular chains was set to zero. The unit cell of the groud-state was stretched and compressed at a strain step of 0.1%. The energy of each step was obtained by fixing the strain and optimizing the unit cell with "opt=ModRedundant".
The cross areas of LPHF, OLPHF, LPBH and OLPBH were difficult to calculate by DFT due to the absence of attractive dispersive forces.[28] The estimated values were listed in Table S1. The width of these macromolecular chains was obtained from the optimized two dimensional structures tiled by macromolecular chains. According to the thickness of PBO, PIPD and graphene, the thicknesses of LPHF, OLPHF, LPBH and OLPBH were estimated to be 0.35 nm.
When calculated the energy curves for PBO and PIPD, the torsion angles between the two ring systems in PBO and PIPD were fixed to be 10^o because the intermolecular forces made the angles in real crystals not zero.[29] This was different from ref.[7] and resulted a relative lower modulus for PIPD (543 GPa). The modulus for PIPD with zero torsion angle was calculated to be 560 GPa, which was very consistent with ref.[7].

Results and discussion

The as-synthesized LPHF is lightweight and dark brown powder with a bulk density as low as 0.035 g cm^{-3} (Fig. 2A) and a BET surface area of 115 m^2 g^{-1} (Fig. S1). Powder X-ray diffraction pattern of the LPHF nanoribbons shows it amorphous structure.
The morphology of the LPHF powder was observed by field-emission scanning electron microscopy (FE-SEM) and shown in Fig. 2B and 2C. The powder is composed predominantly of nanoribbons with few microspheres (Fig. S2). The nanoribbons further tangle up in a random manner to form fluffy aggregates. The enlarged image shows that the width of the nanoribbons are in the range of about 50 ~ 500 nm, while their length and thickness are difficult to be accurately measured.
The aggregates would form during the homogeneous nucleation reaction between hydroquinone and formaledehyde. At the very beginning, large numbers of oligomers formed and uniformly suspended in the solution, afterwards, the oligomers became longer and insoluble. Subsequently, the oligomers assembled with each other and formed short nanoribbons. Finally, the nanoribbons grew longer without significant changes in their width and thickness, which is attributable to the much higher growth rate along the macromolecular chain axis than along the width and thickness directions. The long nanoribbons entangled with each other to form the fluffy aggregates.
The low-magnification TEM image in Fig. 2D shows that no significant contrast can be distinguished in the plane of the belts, which confirms that the ribbon-like morphologies observed in the SEM images are nanoribbons instead of nanofibers. The structure of nanoribbons was further studied by high-resolution transmission electron microscopy (HRTEM), no ordered orientation of macromolecular chains can be observed in the image, most probably due to the fast decomposition of the macromolecular chains resulted from the high energy electron beam irradiation of HRTEM. Instead, ordered arrangement of macromolecular chains can be identified in the HRTEM image (Fig. 2E) of oxidized LPHF (OLPHF). The OLPHF was prepared by oxidizing LPHF with $Ag(NH_3)_2^+$ and the product is a composite of OLPHF and silver nanograins (OLPHF-Ag). The SEM image (Fig. S3) of OLPHF-Ag shows that OLPHF-Ag retains the nanoribbon morphology of the LPHF, while

numerous tiny particles have appeared on the surface of the nanoribbons due to the deposition of silver nanograins (Fig. S4 and S5). The similar nanoribbon morphologies of OLPHF-Ag and LPHF demonstrate that the macromolecular chains of OLPHF-Ag and LPHF are similar in arrangements. Therefore, the macromolecular chains in LPHF would also be in an oriented arrangement, but unfortunately not observable in its TEM image (Fig. S6) due to the carbon chain destruction under the electron beam irradiation.

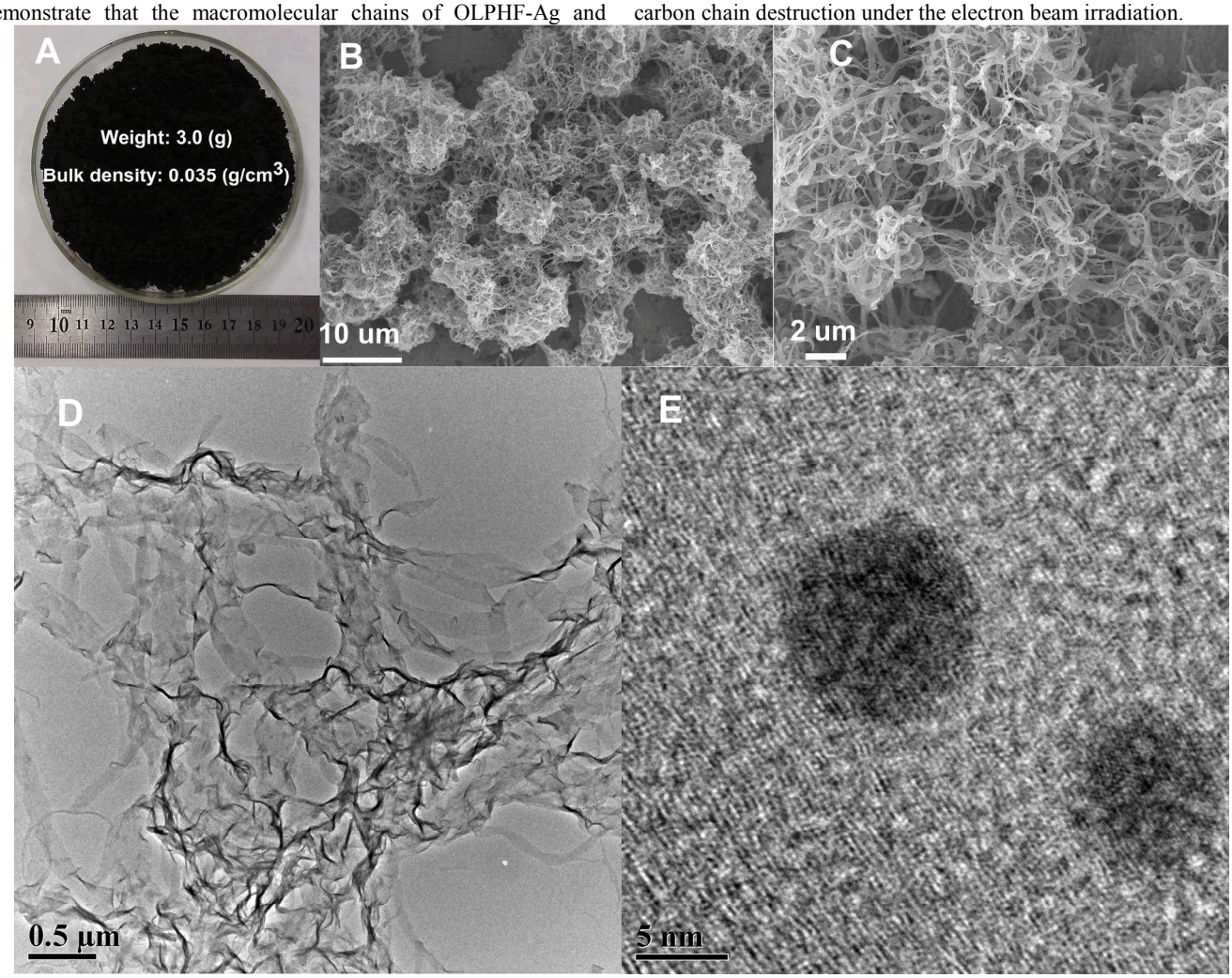

Fig. 2 The digital photo (A), SEM (B, C) and TEM (D, E) images of LPHF, and the HRTEM image (E) of OLPHF-Ag

The chemical formulas of the LPHF and the cylindrical oligomers shown in Fig. 1B are identical with each other, and different from that of the porous polymer because of the presence of $–CH_2OH$ and residual active hydrogen atoms, in the porous polymer.[20] The elemental contents calculated from the chemical formula ($C_8H_6O_2$) of LPHF and cylindrical oligomers are: C 71.64%, H 4.48%, O 23.88%; in comparison to the found results: C 71.27%, H 4.41%. The excellent agreement between the calculated values and the found results excludes the possibility of porous polymers. Further evidence that proves the chemical formula $C_8H_6O_2$ has been found from the silver adsorption experiment. According to the chemical equation in Fig. 3A, the silver adsorption capacity of LPHF has been calculated to be 1.61 g/g resin, which is exactly equal to the experimental adsorption capacity (1.61 g/g resin) calculated from the weight-loss of OLPHF-Ag (Fig. S7). The FT-IR spectra (Fig. S8) of LPHF and OPLHF-Ag show that the C−O stretching bands at 1227 cm^{-1} have been largely weakened after silver adsorption, which demonstrates the substantial conversions of the hydroquinone subunits into quinine subunits during the oxidation reaction.[20]

For the possible products with the chemical formula $C_8H_6O_2$, the LPHF is more likely to be formed than the cylindrical oligomers due to the absence of internal stresses in the structure of LPHF. According to the perfect structure of the ladder polymer (Fig. 1B), only three types of carbons can be distinguished in ^{13}C NMR spectrum. As expected, experimental ^{13}C NMR spectrum shows that there are three strong peaks centered at 149.4, 125.9 and 12.1 ppm (Fig. 4A), which correspond well to the resonances of phenolic, aromatic and methylene carbons,[20, 21] respectively. Besides, there are also two weak peaks centered at 184.0 and 26.5 ppm, which could result from the resonance of carbons on defects. Obviously, the weak peak at 184.0 ppm can be assigned to traces of carbonyl groups resulted from the oxidation of hydroquinone subunit.[21, 30] Owing to the electron withdrawing effect of the carbonyl group, the chemical shifts of methylene group attached directly to the quinone unit would be larger than that of the other methylene groups (12.1 ppm) in LPHF. Therefore, the peak at 26.5 ppm should be assigned to the methylene group attached directly to the quinone unit. After reductive treatment with $NaBH_4$, peaks at 184.0 and 26.5 ppm are both weakened

simultaneously, which also indicates that the two peaks are closely related to the carbonyl group.

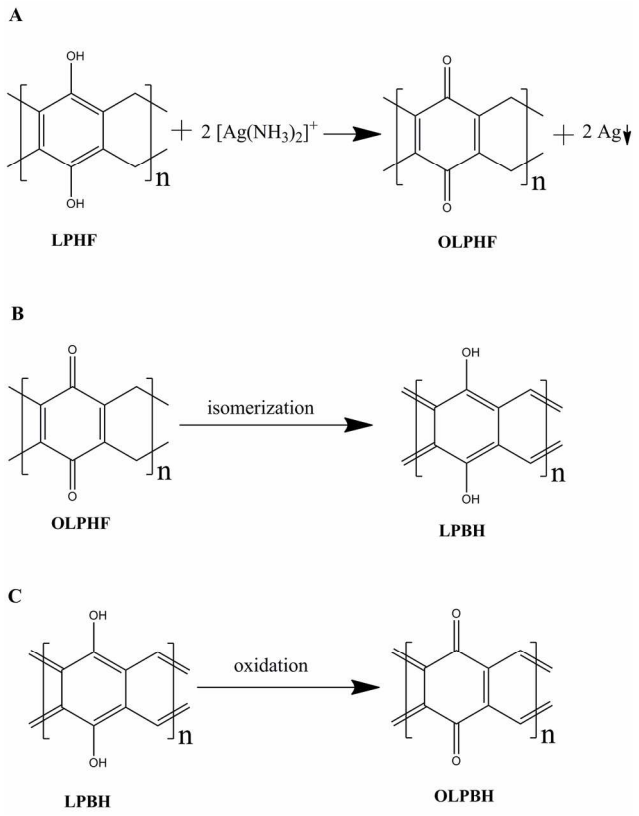

Fig.3 (A) oxidation of LPHF to produce OLPHF. (B) isomerization of OLPHF to produce LPBH. (C) oxidation of LPBH to produce OLPBH.

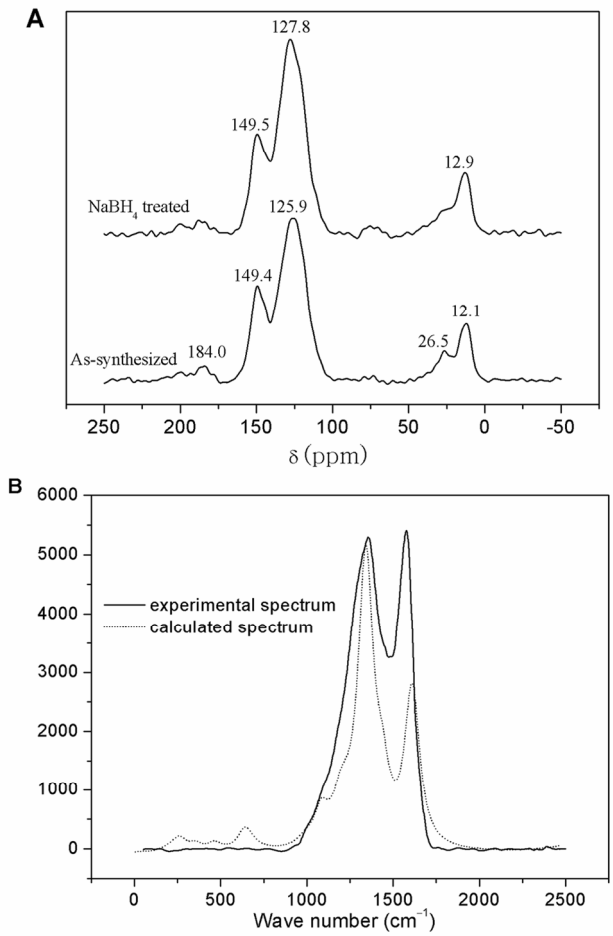

Fig.4 (A) NMR spectra of as-synthesized and $NaBH_4$-treated LPHF. (B) Experimental Raman spectrum of LPHF and calculated Raman spectrum of oligomer with ten hydroquinone units.

For comparison, theoretical calculations of the chemical shifts were performed with Gaussian 09 at Hartree-Fock level of theory using 6-311+G(2d, p) basis sets. Due to the limitation of Gaussian 09, only oligomer extrapolation method can be used for predicting NMR shielding tensors.[31] Hydrogen-ended oligomer with six hydroquinone units (Fig. S9) was selected as the computation model. The calculated chemical shifts were 147.3, 119.4 and 17.3 ppm for phenolic, aromatic and methylene carbons, respectively. These values show good agreement with the experimental results.

Interestingly, the Raman spectrum (Fig. 4B) of LPHF displays two strong lines at 1356 and 1577 cm^{-1}, which are exactly the same as those of graphene except for the broadness of the peaks.[32] Therefore, LPHF could be, to a large extent, regarded as the narrowest (0.73nm) graphene-like structure with its edges modified by definable groups.[32, 33] Again, oligomer extrapolation method was used to predict the Raman spectrum of LPHF.[34] The calculated Raman spectrum of oligomer with ten hydroquinone units shows two strong lines at 1340 and 1605 cm^{-1}, which is in good agreement with the experimental values. The calculation shows that the strongest peak at 1340 cm^{-1} is mainly due to the breathing modes of benzene rings, while the peak at 1605 cm^{-1} can be ascribed to the symmetrical stretching vibrations of benzene rings.

All the above excellent agreements between experiments and calculated results confirm that the polycondensation between hydroquinone and formaldehyde indeed yields a ladder structure fused with six-membered carbon rings.

1,4-benzoquinone and 1,4-cyclohexadiene rings are included in the structure of OLPHF (Fig. 3A). Both of them have a strong tendency to form benzene rings by hydrogenation or dehydrogenation.[35] Therefore, OLPHF can be easily isomerized into fully aromatic structure by a hydrogen transfer reaction (Fig. 3B).[21] The isomerization product was denoted as ladder polymer of benzohydroquinone (LPBH). Quantitatively, Density Functional Theory (DFT) calculations with PBEPBE/6-31G(d) were performed on OLPHF and LPBH.[27] The calculated energy of LPBH is lower than that of OLPHF by 2.1 Kcal/mol structural unit, which indicates that the isomerization of OLPHF is thermodynamically favorable. Therefore, OLPHF is quite likely to be isomerized into LPBH under the excitation of TEM electron beam. The ladder structure of LPBH is identical to that of PAC and has a high structural similarity to graphene nanoribbons.[2, 13, 14] This robust ladder structure of the LPBH makes it stable for a period of time under the electron beam irradiation. As a result, the oriented macromolecular chains shown in Fig. 2E are probably the chains of LPBH. The isomerization reaction shown in Fig.3B presents a possible pathway for synthesizing highly reactive PAC-like polymer. This pathway excludes any side reactions between the highly reactive PAC-like structure and solvents/byproduct.[13]

Due to the reducibility of the hydroquinone units, LPBH could be further oxidized to synthesize a series of intermediate

oxidation products with continuously varied hydrogen contents.[21] The hydrogen contents have a significant effect on the delocalization of the π electron, which in turn modifies the band gaps of the polymers. The band gaps of LPBH and the fully oxidized LPBH (OLPBH in Fig. 3C) were calculated with B3LYP/6-31G(d) on the structures optimized with the same level of theory.[25, 26] The band gaps of LPBH and OLPBH were calculated to be 0.61 and 3.46 eV, respectively. The band gaps of the intermediate products would be within the range of 0.61 ~ 3.46 eV. As expected, the band gap of the hypothetical polymer constructed alternatively with LPBH and OLPBH units (Fig. S10) was similarly calculated to be 2.18 eV (indirect gap) that just fall in the range of 0.61 ~ 3.46 eV.

All of the backbones of the above synthesized polymers have straight ladder-structures constructed with C−C single and C−C double bonds, which qualifies them as high modulus, high strength polymers. Elastic modulus is one of the most important properties for high modulus, high strength polymers. For highly oriented nanoribbon of LPHF and its derivations, their elastic moduli can be assessed at acceptable accuracy by the chain modulus.[7, 36] Using DFT calculations at PBEPBE/6-31G(d) level of theory,[27] the width and the energy curves of these polymers were obtained and shown in Fig. S11 and Fig. S12. The chain moduli (Table. S1) of LPHF, OLPHF, LPBH and OLPBH were calculated to be 528, 536, 620 and 603 GPa, respectively. For comparison, the chain modulus of PE, PBO, PIPD, PAC and CNT(5,5) were similarly calculated to be 309, 530, 543, 745 and 1046 GPa. The results of PE, PBO, PIPD and CNT(5,) are in good agreement with other calculated results and are a little larger than the experiment results,[1, 6, 7, 37, 38] which proves the applicability of the calculation method.

The cross area of LPHF macromolecular chain is estimated to be 0.2555 nm^2 (Table S1), much bigger than those of PBO (0.1982 nm^2) and PIPD (0.2078 nm^2),[7, 39] which leads to a slightly lower modulus of LPHF (528 GPa) as compared with those of PBO (530 GPa) and PIPD (543 GPa). Because of the high rigidity of the fully aromatic structure, the chain modulus of LPBH (620 GPa) is much higher than those of PBO and PIPD, though its cross area (0.2555 nm^2,Table S1) is also bigger than those of PBO (0.1982 nm^2) and PIPD (0.2078 nm^2). In order to evaluate the stiffness of the backbone more accurately, the effects of the variable cross areas on the modulus should be excluded. Because all of these ladder polymers are composed of two zigzag strands of carbon atoms, the cross area of two adjacent zigzag strands in graphite has been chosen as the standard cross area for all of the ladder polymers. The resulting modulus was named as skeleton modulus. The standard cross area calculated from the unit cell parameters of graphite is 0.1448 nm^2.[40] The calculated skeleton moduli for LPHF, OLPHF, LPBH, OLPBH and PAC are 932, 842, 1094, 947 and 1099 GPa, respectively. Obviously, the backbones of PAC and LPBH are the stiffest ones, followed by those of OLPBH and LPHF. The OLPHF has the most flexible ladder structure because there is no rigid benzene ring in the backbone. In particular, the skeleton moduli of LPBH and PAC are slightly larger than that of CNT(5,5) (1046 GPa), which is resulted from the fact that the C−C bonds in the strands of LPBH (0.141 nm) and PAC (0.141 nm) are slightly shorter and stiffer than those in CNT(5,5) (0.143 nm).

Conclusions

In summary, we have demonstrated the facile synthesis of an all-carbon ladder polymer from a one-pot polycondensation reaction between hydroquinone and formaldehyde. This polymer can be further oxidized and isomerized to other all-carbon ladder polymers without change in its backbone structure, which paves the way for synthesizing PAC-like ladder polymer. The chain moduli and sckeleton moduli of these polymers have been calculated by DFT method. These calculated moduli are among the highest in the synthetic polymers. The nanoribbon morphology qualifies theif application in reinforcing other polymer matrices. The energy band structures of these polymers could be modulated by changing hydrogen contents of the ladder structure, which makes these polymers suitable candidates for application in molecular devices, sensors and even all-organic solar cells.

Acknowledgements

This work was supported by Natural Science Foundation of China (51132009) and China Postdoctoral Science Foundation (2011M501042).

Notes and references

[a] Chery Automobile Co. Ltd; 8 Chang-chun road, Wuhu 241006, Anhui, China.
[b] Gansu Computing Center, Lanzhou 730030, Gansu, China.
[c] Suzhou Institute of Nano-tech and Nano-bionics, Chinese Academy of Sciences, 398 Ruoshui road, Suzhou 215123, China.
[d] State Key Laboratory of High-Performance Ceramics and Superfine Microstructures, Shanghai Institute of Ceramics, Chinese Academy of Sciences, 1295 Ding-xi Road, Shanghai 200050, China.
E-mail: jlshi@sunm.shcnc.ac.cn; Tel:+86-021-52411088
Electronic Supplementary Information (ESI) available: [Nitrogen isotherms, SEM and TEM images, TG-DTA curves, FT-IR spectra, Schematics, and Table of moduli]. See DOI: 10.1039/b000000x/

1. M. M. Shokrieh and R. Rafiee, Mater. Des., 2010, 31, 790-795.
2. J. Cai, P. Ruffieux, R. Jaafar, M. Bieri, T. Braun, S. Blankenburg, M. Muoth, A. P. Seitsonen, M. Saleh, X. Feng, K. Mullen and R. Fasel, Nature, 2010, 466, 470-473.
3. D. V. Kosynkin, A. L. Higginbotham, A. Sinitskii, J. R. Lomeda, A. Dimiev, B. K. Price and J. M. Tour, Nature, 2009, 458, 872-876.
4. C. Lee, X. Wei, J. W. Kysar and J. Hone, Science, 2008, 321, 385-388.
5. X. Li, X. Wang, L. Zhang, S. Lee and H. Dai, Science, 2008, 319, 1229-1232.
6. R. J. Davies, S. J. Eichhorn, C. Riekel and R. J. Young, Polymer, 2004, 45, 7693-7704.
7. J. C. L. Hageman, J. W. van der Horst and R. A. de Groot, Polymer, 1999, 40, 1313-1323.
8. U. Scherf, J. Mater. Chem., 1999, 9, 1853-1864.
9. A. D. Schluter, M. Loffler and V. Enkelmann, Nature, 1994, 368, 831-834.

10. U. Scherf and K. Müllen, Synthesis and Photosynthesis, Springer Berlin Heidelberg, 1995, vol. 123, ch. 1, pp. 1-40.
11. M. B. Goldfinger and T. M. Swager, J. Am. Chem. Soc., 1994, 116, 7895-7896.
12. J. Jacob, S. Sax, T. Piok, E. J. W. List, A. C. Grimsdale and K. Müllen, J. Am. Chem. Soc., 2004, 126, 6987-6995.
13. S. Kivelson and O. L. Chapman, Phys. Rev. B, 1983, 28, 7236-7243.
14. K. N. Houk, P. S. Lee and M. Nendel, J. Org. Chem., 2001, 66, 5517-5521.
15. C. Tönshoff and H. F. Bettinger, Angew. Chem. In. Ed., 2010, 49, 4125-4128.
16. B. Schlicke, H. Schirmer and A.-D. Schlüter, Adv. Mater., 1995, 7, 544-546.
17. J. K. Stille and E. L. Mainen, Macromolecules, 1968, 1, 36-42.
18. M. Imoto, I. Ijichi, C. Tanaka and M. Kinoshita, Makromol. Chem., 1968, 113, 117-130.
19. C. D. Gutsche, Acc. Chem. Res., 1983, 16, 161-170.
20. S. Zeng, L. Guo, L. Zhang, F. Cui, J. Zhou, Z. Gao, Y. Chen and J. Shi, Macromol. Chem. Phys., 2010, 211, 845-853.
21. V. F. Dalal, M. H. Litt and S. E. Rickert, J. Polym. Sci.: Polym. Chem. Ed., 1985, 23, 2659-2668.
22. S. Brunauer, P. H. Emmett and E. Teller, J. Am. Chem. Soc., 1938, 60, 309-319.
23. M. J. Frisch, G. W. Trucks, H. B. Schlegel, et al., Gaussian 09, Revision C.01, Gaussian, Inc., Wallingford CT, 2010.
24. W. Dixon, J. Schaefer, M. Sefcik, E. Stejskal and R. McKay, J. Magn. Reson., 1982, 49, 341-345.
25. A. D. Becke, J. Chem. Phys., 1993, 98, 5648-5652.
26. C. Lee, W. Yang and R. G. Parr, Phys. Rev. B, 1988, 37, 785-789.
27. J. P. Perdew, K. Burke and M. Ernzerhof, Phys. Rev. Lett., 1996, 77, 3865-3868.
28. E. J. Meijer and M. Sprik, J. Chem. Phys., 1996, 105, 8684-8689.
29. E. A. Klop and M. Lammers, Polymer, 1998, 39, 5987-5998.
30. Y. Morita, T. Agawa, E. Nomura and H. Taniguchi, J. Org. Chem., 1992, 57, 3658-3662.
31. P. S. Asirvatham, V. Subramanian, R. Balakrishnan and T. Ramasami, Macromolecules, 2003, 36, 921-927.
32. K. N. Kudin, B. Ozbas, H. C. Schniepp, R. K. Prud'homme, I. A. Aksay and R. Car, Nano Lett., 2007, 8, 36-41.
33. T. Szabó, O. Berkesi, P. Forgó, K. Josepovits, Y. Sanakis, D. Petridis and I. Dékány, Chem. Mater., 2006, 18, 2740-2749.
34. M. I. Boyer, S. Quillard, E. Rebourt, G. Louarn, J. P. Buisson, A. Monkman and S. Lefrant, J. Phys. Chem. B, 1998, 102, 7382-7392.
35. F. Stoos and J. Rocek, J. Am. Chem. Soc., 1972, 94, 2719-2723.
36. B. Crist, Ann. Rev. Mater. Sci., 1995, 25, 295-323.
37. J. C. L. Hageman, R. J. Meier, M. Heinemann and R. A. de Groot, Macromolecules, 1997, 30, 5953-5957.
38. M. Lammers, E. A. Klop, M. G. Northolt and D. J. Sikkema, Polymer, 1998, 39, 5999-6005.
39. A. V. Fratini, P. G. Lenhert, T. J. Resch and W. W. Adams, MRS Online Proceedings Library, 1988, 134, null.
40. L. Pauling, PNAS, 1966, 56, 1646.